Robust Object Tracking by Nonlinear Learning

Bo Ma, Hongwei Hu, Jianbing Shen, *Senior Member, IEEE*, Yuping Zhang,
Ling Shao, *Senior Member, IEEE*, and Fatih Porikli, *Fellow, IEEE*

***Abstract*— We propose a method that obtains a discriminative visual dictionary and a nonlinear classifier for visual tracking tasks in a sparse coding manner based on the globally linear approximation for a nonlinear learning theory. Traditional discriminative tracking methods based on sparse representation learn a dictionary in an unsupervised way and then train a classifier, which may not generate both descriptive and discriminative models for targets by treating dictionary learning and classifier learning separately. In contrast, the proposed tracking approach can construct a dictionary that fully reflects the intrinsic manifold structure of visual data and introduces more discriminative ability in a unified learning framework. Finally, an iterative optimization approach, which computes the optimal dictionary, the associated sparse coding, and a classifier, is introduced. Experiments on two benchmarks show that our tracker achieves a better performance compared with some popular tracking algorithms.**

***Index Terms*—Global linear approximation, local coordinate coding (LCC), nonlinear learning, object tracking.**

I. Introduction

Visual tracking is a popular topic in computer vision, and numerous tracking methods [1]–[3], [26], [43], [54] have been proposed to deal with challenges, such as illumination variation [12], [16], global or partial occlusion, shape deformation, in-plane rotation, and background clutters. To evaluate the performance of different tracking algorithms quantitatively, several tracking data sets, such as visual tracking benchmark [4] and VOT2014 [5], have been established.

Among current tracking approaches, much attention has been attracted by sparse representation-based approaches because of their robust performances in vision tasks [6], [36], [41]. Many sparse coding-based tracking methods [7] have been proposed by researchers. Broadly speaking, a given candidate sample can be encoded by a linear combination of a few atoms spanning an overcomplete dictionary that is learned from a training set of samples in sparse coding-based methods. Different dictionary learning approaches [8]–[10], [47], [49], [52], [55] based on sparse coding have been proposed for signal reconstruction and classification in the audio and image processing domains. In visual tracking, the learning and updating of a dictionary are crucial steps to handle and adapt to appearance variation during tracking procedure as well. Therefore, a suitable dictionary selection carries significant importance. Mei and Ling [11] constructed a dictionary to encode the candidate targets by employing the global target templates. Bao *et al.* [13] introduced the accelerated proximal gradient approach to promote the real time l_1 tracker with the same dictionary learning strategy. Zhong *et al.* [14] introduced a sparsity-based collaborative model with a generative and a discriminative model. The discriminative classifier was trained by a dictionary with holistic templates, while the generative model was based on a local dictionary from local patches by k-means. This method performs well under drastic appearance changing. Most sparse coding-based discriminative object tracking methods [15] learn dictionary and train classifier using a separated mechanism. To acquire the dictionary for coding, some unsupervised clustering methods, such as k-means, are usually adopted, but the produced dictionary may not be suitable for tracking task. Yang *et al.* [17] proposed an online discriminative dictionary learning approach for visual tracking. But this method leaves the locality of sparse codes out, and has no consideration on the underlying manifold geometry structure of neither labeled samples nor unlabeled samples during dictionary learning.

A classification function learning using visual data is restricted to be nonlinear as a necessity because of the target appearance variation during the tracking process. In principle, the so-called "curse of dimensionality" may arise due to high-dimensional feature for modeling target appearance changing. This phenomenon is seldom observed during a practical tracking procedure. Moreover, a satisfying tracking performance could be obtained using only a handful of visual training samples. One possible reason is that typically, visual data represented by high-dimensional vectors reside in a low dimensionality embedding manifold of the high-dimensional space that they lie in. Based on this inference, a nonlinear learning theory using local coordinate coding (LCC) is proposed in [18] and [19]. LCC is a general coding framework that approximates any nonlinear Lipschitz smooth function using linear functions. It consists of a sparse coding scheme that

Manuscript received January 17, 2017; revised April 20, 2017 and July 24, 2017; accepted November 10, 2017. This work was supported in part by the National Natural Science Foundation of China under Grant 61472036, Grant 61272359, Grant 61672099, and Grant 81627803, in part by the National Key Research and Development Program of China under Grant 2017YFC0112000, in part by the Australian Research Council's Discovery Projects Funding Scheme under Grant DP150104645, in part by the Fok Ying-Tong Education Foundation for Young Teachers, and in part by the Joint Building Program through the Beijing Municipal Education Commission. *(Corresponding author: Jianbing Shen.)*

B. Ma, H. Hu, J. Shen, and Y. Zhang are with the Beijing Laboratory of Intelligent Information Technology, School of Computer Science and Technology, Beijing Institute of Technology, Beijing 100081, China (e-mail: bma000@bit.edu.cn; shenjianbing@bit.edu.cn).

L. Shao is with JD Artificial Intelligence Research, Beijing 100176, China, and also with the School of Computing Sciences, University of East Anglia, Norwich NR4 7TJ, U.K. (e-mail: ling.shao@uea.ac.uk).

F. Porikli is with the Research School of Engineering, Australian National University, Canberra ACT 0200, Australia (e-mail: fatih.porikli@anu.edu.au).

Color versions of one or more of the figures in this paper are available online at http://ieeexplore.ieee.org.

Digital Object Identifier 10.1109/TNNLS.2017.2776124

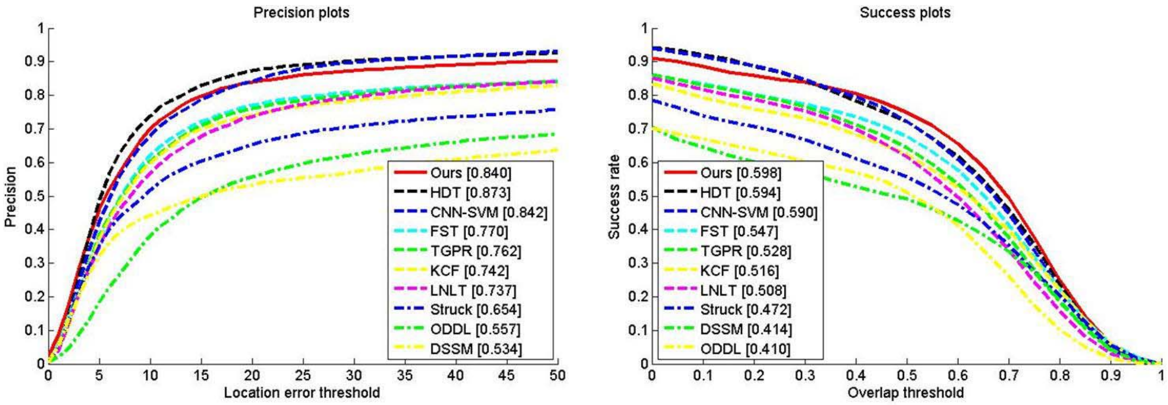

Fig. 1. Overall performance comparisons of precision plots (left) and success rates (right) for these trackers. The overall performance scores at 20 pixels are presented in the legend.

defines the local coordinates and a dictionary that contains the local coordinates. It shows that under some Lipschitz continuity assumption, the computational complexity for learning a nonlinear classification function relies on the dimensionality of inherent manifold sample space. Considering the manifold geometry structure of sample space, we think that those dictionary items close to samples to be encoded should be activated. LCC could keep locality of codes while reconstructing original samples using the learned dictionary items. Impressive performance is exhibited on nonlinear learning using LCC [20]. It also shows high classification accuracies on large-scale image classification [21] and object recognition [22], [24]. However, those methods formulate their visual dictionary with a simple unsupervised way. And they all treat dictionary learning and classifier learning as a separated way, and take a two-stage learning strategy. It may not generate an optimal dictionary that owns discriminative power and reflects the spatial geometry structure of sample space. Even so, the nonlinear theory using LCC endows a firm theoretical foundation to promote the sparse coding-based discriminative visual tracking algorithm.

In this paper, we present a well-designed tracking algorithm that aims to learn visual dictionary and nonlinear classification function jointly enlighten by the above-mentioned nonlinear learning theory under a semisupervised framework. The dictionary is learned to describe the embedded manifold structure constructed by samples with and without labels, and it is also expected to maintain approving discriminative power. Therefore, the proposed method could overcome several limitations arisen in most of the existing visual tracking approaches efficiently. Furthermore, it employs the localized sparse representation to provide the guidance for discriminative visual tracking, which has a solid theoretical basis. The final discriminative dictionary, classification function, and sparse codes are calculated by an iterative optimization algorithm. One preliminary version of this paper was presented in [23], and this paper is significantly different. First, more theoretical foundations about the theory of globally linear approximation to nonlinear learning are introduced (see Section II-A). Second, the theoretical analysis of each item is added and explained concretely, such as the semisupervised learning item (3) and the discriminative item (4). Third, a new analysis about the relationships between the classifier and the learned dictionary in our optimization algorithm is explained in Section II-B. Fourth, drifting often occurs during long-term tracking due to occlusion and deformation in many tracking tasks. In order to alleviate this issue, a target redetection method is introduced to relocate target once tracking fails (see Section III-D). Fifth, a center refining scheme is introduced in the experiments (see Section IV-A) to further improve the tracking performance. Finally, we compare this paper with more recent tracking methods on OTB2013 (see Fig. 1 and Table I). And more experimental analysis (see Section IV-C) and experiments on visual object tracking challenge 2015 (VOT2015) (see Fig. 2) are added as well. Our source code will be available online.[1]

II. Globally Linear Approximation to Nonlinear Learning

A. Problem Description

Given a set of labeled samples $X_l = \{\mathbf{x_1}, \ldots, \mathbf{x_n}\}$ with their labels $Y = \{y_1, \ldots, y_n\}$, where $\mathbf{x_i} \in \mathbb{R}^{\mathbf{d}}$ and a group of unlabeled samples $X_u = \{\mathbf{x_{n+1}}, \ldots, \mathbf{x_{n+u}}\}$, our goal is to learn a nonlinear classification function, a discriminative dictionary, and sparse coefficients for samples represented under dictionary. We aim to learn a nonlinear classifier on a very high-dimensional sample space originated from visual tracking problem. In view of the traditional statistical theory, the performance decreases when dimensionality of sample feature exceeds an optimal number. Thus, learning a nonlinear function from this sample space is inaccurate. Fortunately, the theory of globally linear approximation to nonlinear learning shows that a nonlinear function $f(\mathbf{x})$ could be approximated by a linear function with regard to local coordinate coefficients of samples under manifold assumption [18]

$$\left| f(\mathbf{x}) - \sum_{i=1}^{|\mathbf{D}|} \alpha_i f(\mathbf{d}_i) \right| \le \beta \|\mathbf{x} - \gamma(\mathbf{x})\| + \delta \sum_{i=1}^{|\mathbf{D}|} |\alpha_i| \|\mathbf{d}_i - \gamma(\mathbf{x})\|^{1+p} \quad (1)$$

[1] http://github.com/shenjianbing/LLCtracking.

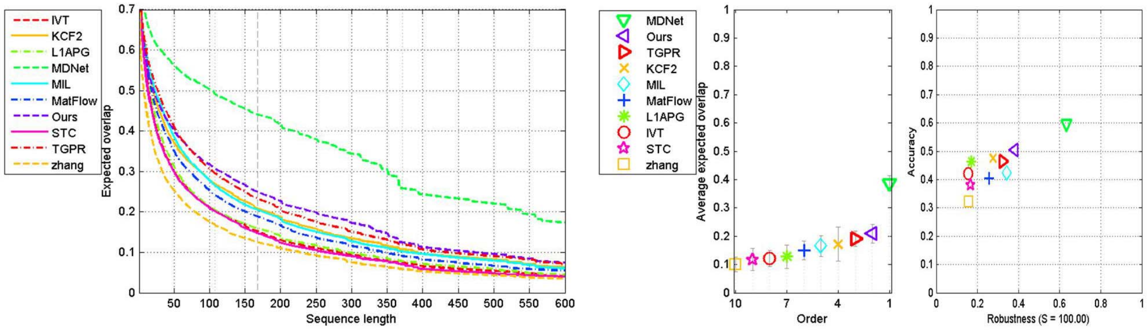

Fig. 2. Results on VOT2015. Left: expected overlap curves. Middle: expected overlap graph with the ranked trackers. The right-most tracker is the top-performing according to the VOT2015 expected average overlap values. The horizontal axis denotes the orders of different trackers. Right: accuracy robustness (AR) plot for experiment baseline, where the sensitive $S = 100$. For more details, please refer to [31].

where $\gamma(\mathbf{x}) = \mathbf{D}\boldsymbol{\alpha}$, $\mathbf{D} = [\mathbf{d}_1, \ldots, \mathbf{d}_m] \in \mathbb{R}^{d\times m}$ is the dictionary, and $\boldsymbol{\alpha}$ is the code of sample $\mathbf{x}$. This equation means that a very high-dimensional nonlinear learning problem can be translated into a much simpler linear learning problem. By minimizing the upper bound, we could obtain a much simpler approximated linear function with the codes of original samples as its input instead of original complicated nonlinear function. The upper bound of the approximation error is bounded by the reconstruction error of a sample and the affinity between the sample and dictionary items. For a sample $\mathbf{x}_i$, LCC, which is just the upper bound, is approximated as

$$\begin{aligned}&\min_{\mathbf{D},\boldsymbol{\alpha}_i} \|\mathbf{x}_i - \mathbf{D}\boldsymbol{\alpha}_i\|^2 + \mu \sum_{j=1}^{m} \left|\alpha_i^j\right| ||\mathbf{d}_j - \mathbf{x}_i||^2\\ &\text{s.t. } \mathbf{1}^T\boldsymbol{\alpha}_i = 1 \end{aligned} \quad (2)$$

where μ is a constant factor to balance reconstruction error and locality, α_i^j denotes the jth element of $\boldsymbol{\alpha}_i$, which is the local coordinate code of sample $\mathbf{x}_i$ under dictionary $\mathbf{D}$, and each element in vector $\mathbf{1}$ is a set to one.

Considering both labeled and unlabeled samples, we extend (2) as

$$\begin{aligned}&\min_{\mathbf{D},\mathbf{A}} \sum_{i=1}^{u+n} \left(\|\mathbf{x}_i - \mathbf{D}\boldsymbol{\alpha}_i\|^2 + \mu \sum_{j=1}^{m} \left|\alpha_i^j\right| ||\mathbf{d}_j - \mathbf{x}_i||^2 \right)\\ &\text{s.t. } \mathbf{1}^T\boldsymbol{\alpha}_i = 1, \quad i = 1, \ldots, n+u. \end{aligned} \quad (3)$$

We denote $\mathbf{A} = [\boldsymbol{\alpha}_1, \ldots, \boldsymbol{\alpha}_{n+u}] \in \mathcal{R}^{m\times(n+u)}$ as the code matrix of all training samples. The locality of LCC brings sparsity, but it is not true contrarily. The globally linear approximation of $f(\mathbf{x}_i)$ is formulated as $f(\mathbf{x}_i) \approx \boldsymbol{\alpha}_i^T\mathbf{w}$ under the nonlinear learning theory using LCC. And the labeled samples should be considered for discriminative dictionary learning. Therefore, we introduce the discriminative item as

$$\min_{\mathbf{W},\mathbf{A}_l} \|\mathbf{A}_l^T\mathbf{w} - \mathbf{y}\|^2, \quad \text{s.t. } \mathbf{1}^T\boldsymbol{\alpha}_i = 1,\ i = 1, \ldots, n \quad (4)$$

where code matrix $\mathbf{A}_l = [\boldsymbol{\alpha}_1, \ldots, \boldsymbol{\alpha}_n]$ corresponds to the labeled samples.

We intend to assign similar labels to those neighbor samples considering the geometry spatial structure constructed by samples. In LCC, a sample could be sparsely constructed by the bases in advance with a linear combination manner, such as other sparse coding approaches. For simplicity, a novel sparse coding method is introduced as an approximation of LCC [21]. It encodes a sample with k dictionary items, which are the nearest neighbors of the sample. And the corresponding sparse code is obtained by solving a least squares problem with some equality constraints. It will reach our objective obviously, since neighbor samples will be encoded by several same dictionary items. Therefore, we introduce a Laplacian regularization item to handle it. More theoretical analysis about Laplacian regularization refers to [25]. Finally, the proposed semisupervised learning method for dictionary, sparse codes, and classification function is formulated as

$$\begin{aligned}&\min_{\mathbf{D},\mathbf{A},\mathbf{w}} \sum_{i=1}^{u+n} \left(\|\mathbf{x}_i - \mathbf{D}\boldsymbol{\alpha}_i\|^2 + \mu \sum_{j=1}^{m} \left|\alpha_i^j\right| ||\mathbf{d}_j - \mathbf{x}_i||^2 \right)\\ &\qquad + \lambda_1 \left\|\mathbf{A}_l^T\mathbf{w} - \mathbf{y}\right\|^2 + \lambda_2 \sum_{i=1}^{n+u}\sum_{j=1}^{n+u} \left\|\boldsymbol{\alpha}_i^T - \boldsymbol{\alpha}_j^T\mathbf{w}\right\|^2 B_{ij}\\ &\text{s.t. } \mathbf{1}^T\boldsymbol{\alpha}_i = 1, \quad i = 1, \ldots, n+u \end{aligned} \quad (5)$$

where the last item is the Laplacian constraint with $B_{ij} = \boldsymbol{\alpha}_i^T\boldsymbol{\alpha}_j$ and λ_1 and λ_2 are two preset constants that balance the discriminative ability and manifold spatial constraint.

Manifold regularization has been used in several earlier works [51]. But there are significant differences between our method and [51] and [53]. First, our method aims to track a single general object in one video clip, while [51] performs tracking for multiple persons in multiple videos using person detection and face recognition techniques. Thus, these two methods belong to different topics of visual tracking tasks. Second, our tracking method is solved as a regression problem, and the label of a sample is represented by a regression value, while the label of sample in [51] is represented by a label vector, and the tracking problem is treated as a multiclass classification problem. Third, the proposed optimization algorithm utilizes a linear regression model with respect to LCC codes of samples to predict the labels of samples. The linear regression model is a globally linear approximation of original nonlinear function under the nonlinear learning theory using LCC. But [51] and [53] predict the labels vectors of data points using a linear regression model with respect to original samples, which does not satisfy the basic theory assumption of our approach. All the Laplacian matrices in our method and theirs consider the manifold structure of samples, and the main idea behind them assumes that neighbor samples should have similar labels. However, the Laplacian matrix in our method includes a variable (sparse code matrix A) to be solved iteratively, while the Laplacian matrices in [51] and [53] are constant matrices. Additionally, the distance between different samples [B_{ij} in (5)] in our method has been continuously updated during the iteration. The learned sparse code for each sample reflects its real spatial position in the manifold space according to both discriminative information and local geometry structures of all data points. The optimization algorithm of the proposed model is introduced in Section II-B, and the proposed algorithm is summarized in Algorithm 1.

Algorithm 1 Proposed Learning Algorithm

```
Input: ${(\mathbf{x}_i, y_i)}_{i=1}^{n}$, ${\mathbf{x}_i}_{i=n+1}^{n+u}$, $\mu$, $\lambda_1$ and $\lambda_2$.
Output: $\mathbf{D}$, $\mathbf{A}$ and $\mathbf{w}$.
Initialization: $\mathbf{D}$ is achieved using $k$-means algorithm, $\mathbf{A}_l = (\mathbf{D}^T\mathbf{D})^{-1}(\mathbf{D}^T\mathbf{X})$, and $\mathbf{X} = [\mathbf{x}_1, \dots, \mathbf{x}_{n+u}]$.
$t = 1$;
while $t < T$ do
    Classifier learning: Solve $\mathbf{w}$ using (7) with fixed $\mathbf{D}$, $\mathbf{A}$;
    Coding: Solve $\mathbf{A}$ by Algorithm 2 with fixed $\mathbf{D}$, $\mathbf{w}$;
    Dictionary learning: Learn $\mathbf{D}$ with fixed $\mathbf{A}$, $\mathbf{w}$ by (17);
    $t = t + 1$.
end while
```

B. Optimization Algorithm

Equation (5) could be solved directly, since it is not convex jointly over variables **D**, **w**, and **A**. In this paper, we seek to optimize one variable while fixing the other two ones. To this end, the objective function is decomposed into three subproblems, and the optimal results will be acquired using an iterative way.

1) Subproblem A (Classifier Learning): By fixing dictionary **D** and sparse code matrix **A**, the following optimization problem is presented to learn classification function:

$$\min_{\mathbf{w}} \ \lambda_1 \left\| \mathbf{A}_l^T \mathbf{w} - \mathbf{y} \right\|^2 + \lambda_2 \sum_{i=1}^{n+u} \sum_{j=1}^{n+u} \left\| \boldsymbol{\alpha}_i^T \mathbf{w} - \boldsymbol{\alpha}_j^T \mathbf{w} \right\|^2 B_{ij}$$
$$\text{s.t. } \mathbf{1}^T \boldsymbol{\alpha}_i = 1, \quad i = 1, \dots, n. \tag{6}$$

The optimal solution of **w** could be achieved by setting the derivative of (6) to zero. And the final closed-form solution is calculated as

$$\mathbf{w} = \left(\lambda_1 \mathbf{A}_l \mathbf{A}_l^T + \lambda_2 \mathbf{A}(\Delta - \mathbf{A}^T \mathbf{A})\mathbf{A}^T\right)^{-1} (\lambda_1 \mathbf{A}_l \mathbf{y}) \tag{7}$$

where $\Delta = \text{diag}(\Delta_1, \Delta_2, \dots, \Delta_{u+n})$ with $\Delta_i = \sum_{j=1}^{u+n} B_{ij}$.

2) Subproblem B (Coding): To obtain the sparse codes matrix **A**, we solve the objective function with **D** and **w** fixed. In fact, the resulting minimization problem is just (5). But it could not be solved directly by derivation, since this function is nondifferentiable with regard to sparse codes matrix. Thus, locality-constrained linear coding [20] is introduced as an approximate formulation of (5), which could be solved analytically. In this paper, we neglect the Laplacian regularization term here for simplicity. Let $\mathbf{c}_i = [c_i^1, \dots, c_i^m]^T$, where $c_i^j = \|\mathbf{x}_i - \mathbf{d}_j\|$ denotes the Euclidean distance between dictionary entry $\mathbf{d}_j$ and sample $\mathbf{x}_i$. The approximated minimization problem could be formulated as

$$\min_{\mathbf{A}} \sum_{i=1}^{u+n} \left(\|\mathbf{x}_i - \mathbf{D}\boldsymbol{\alpha}_i\|^2 + \mu \|\mathbf{c}_i \odot \boldsymbol{\alpha}_i\|^2 \right) + \lambda_1 \left\| \mathbf{A}_l^T \mathbf{w} - \mathbf{y} \right\|^2$$
$$\text{s.t. } \mathbf{1}^T \boldsymbol{\alpha}_i = 1, \quad i = 1, \dots, n + u \tag{8}$$

where $\odot$ represents the Hadamard product. This minimization problem could be solved by calculating one column of **A** with fixed others. The solving procedure is iterated until convergence. Then, each $\boldsymbol{\alpha}_i$ could be calculated analytically with a closed-form solution

$$\boldsymbol{\alpha}_i = \mathbf{P}^{-1} \left(\mathbf{Q} - \frac{\mathbf{1}^T \mathbf{P}^{-1} \mathbf{Q} \mathbf{1} - 1}{\mathbf{1}^T \mathbf{P}^{-1} \mathbf{1}} \mathbf{1} \right). \tag{9}$$

For the $\boldsymbol{\alpha}_i$ values corresponding to sample $\mathbf{x}_i$ values with labels

$$\mathbf{P} = \mathbf{D}^T \mathbf{D} + \mu \text{diag}\left(\mathbf{c}_i^2\right) + \lambda_1 \mathbf{w}\mathbf{w}^T \tag{10}$$
$$\mathbf{Q} = \mathbf{D}^T \mathbf{x}_i + \lambda_1 \mathbf{w} y_i \tag{11}$$

where $(c_i^j)^2$ is the jth element of diagonal matrix $\text{diag}(\mathbf{c}_i^2)$. For those $\boldsymbol{\alpha}_i$ values corresponding to samples without labels

$$\mathbf{P} = \mathbf{D}^T \mathbf{D} + \mu \text{diag}\left(\mathbf{c}_i^2\right) \tag{12}$$
$$\mathbf{Q} = \mathbf{D}^T \mathbf{x}_i. \tag{13}$$

The detailed derivation of subproblem A is given in Appendix A. Algorithm 2 summarizes the proposed coding algorithm.

Algorithm 2 Coding Algorithm

```
Input: ${(\mathbf{x}_i, y_i)}_{i=1}^{n}$, ${\mathbf{x}_i}_{i=n+1}^{n+u}$, $\mu$, $\lambda_1$, $\mathbf{D}$ and $\mathbf{w}$.
Output: A
$t = 1$;
while $t < T$ do
    for $i = 1 : n + u$ do
        $\mathbf{P} = \mathbf{D}^T\mathbf{D} + \mu \text{diag}(\mathbf{c}_i^2)$;
        $\mathbf{Q} = \mathbf{D}^T\mathbf{x}_i$;
        if $i \le n$ then
            $\mathbf{P} = \mathbf{P} + \lambda_1 \mathbf{w}\mathbf{w}^T$;
            $\mathbf{Q} = \mathbf{Q} + \lambda_1 \mathbf{w} y_i$;
        end if
        $\boldsymbol{\alpha}_i = \mathbf{P}^{-1}\left(\mathbf{Q} - \frac{\mathbf{1}^T\mathbf{P}^{-1}\mathbf{Q}\mathbf{1}-1}{\mathbf{1}^T\mathbf{P}^{-1}\mathbf{1}}\mathbf{1}\right)$;
    end for
    $t = t + 1$.
end while
```

3) Subproblem C (Dictionary Learning): To learn the dictionary **D**, we aim to minimize the following problem with fixed **A** and **w**:

$$\min_{\mathbf{D}} \sum_{i=1}^{u+n} \left(\|\mathbf{x}_i - \mathbf{D}\boldsymbol{\alpha}_i\|^2 + \mu \sum_{j=1}^{m} \left|\alpha_i^j\right| \left\|\mathbf{d}_j - \mathbf{x}_i\right\|^2 \right).$$

After derivation (refer to [22] for more details), the above minimization problem is equivalent to

$$\min_{\mathbf{D}} \operatorname{tr}(\mathbf{D}^T\mathbf{D}\mathbf{G}) - 2\operatorname{tr}(\mathbf{D}^T\mathbf{S}) \tag{14}$$

$$\mathbf{G} = \sum_{i=1}^{n+u} \left(\boldsymbol{\alpha}_i\boldsymbol{\alpha}_i^T + \mu\operatorname{diag}(|\boldsymbol{\alpha}_i|)\right) \tag{15}$$

$$\mathbf{S} = \sum_{i=1}^{n+u} \left(\mathbf{x}_i\boldsymbol{\alpha}_i^T + \mu\mathbf{x}_i|\boldsymbol{\alpha}_i|^T\right) \tag{16}$$

where the trace operator $\operatorname{tr}(\cdot)$ acts on a square matrix. The block-coordinate descent algorithm in [22] can be a viable approach to obtain the optimal dictionary. But in this paper, it exists a closed-form formulation, which could be written as

$$\mathbf{D} = \mathbf{S}\mathbf{G}^{-1}. \tag{17}$$

The detailed derivation of subproblem B is given in Appendix B. Actually, the dictionary entry could be regarded as a labeled item, and the sign of its corresponding element in classifier $\mathbf{w}$ is just its label.

III. Tracking Approach

A. Samples Collection

Generally, the initial state of an interesting object in tracking methods is annotated in the first frame manually. In this paper, we crop a group of holistic templates $\{\mathbf{x}_i\}_{i=1}^n$ within a certain scope of the object region randomly according to a Gaussian distribution as the labeled samples. Most discriminative visual tracking methods are usually seen as a binary classification problem, and the label of each sample is annotated as a discrete value, such as 0 or 1. For more accurate annotation, we set the labels of samples using continuous values, which lie in [0, 1] in our method. The label of a sample $\mathbf{x}_i$ is computed as

$$y_i = \frac{\mathrm{Ar}_s \cap \mathrm{Ar}_t}{\mathrm{Ar}_s \cup \mathrm{Ar}_t} \tag{18}$$

where Ar_t is the area of object region and Ar_s is the area of a template. It is observed that the similarity between the target and the sample increases with the rise of the sample label value. The value of the label is 1 for a sample overlapped with the target region completely, and 0 if no overlap exists between them. It is reasonable, because the samples drifting from the target are between target and nontarget, and we could not assign them to 1 or 0 crudely. Thus, continuous labels are a good choice.

The optimization of (5) needs n labeled samples and u unlabeled samples, and we assign similar labels for neighbor samples in the manifold space. Thus, unlabeled samples are also needed to the proposed method. The target candidates $\{\mathbf{x}_i\}_{i=n+1}^{n+u}$ selected in the current frame within a certain scope of the previous target state are treated as unlabeled ones. Then, we train a classifier to assign labels for target candidates using all these samples in an online manner.

B. Confidence Calculation

The training samples containing labeled and unlabeled ones collected in Section III-A will be utilized to train the proposed model in (5), and then, the optimal dictionary $\mathbf{D}$, LCC matrix $\mathbf{A}$ of samples, and the linear classifier $\mathbf{w}$ will be obtained. The regression value of a target candidate $\mathbf{x}_i$ is calculated as $f(\mathbf{x}_i) = \boldsymbol{\alpha}_i^T\mathbf{w}$, where $\boldsymbol{\alpha}_i$ is the LCC of $\mathbf{x}_i$. It measures the affinity similarity of a candidate target to real object. Thus, we could obtain all the confidences of candidates.

Nevertheless, only global template considered in tracking is inadequate to cope with partial occlusion problem arisen in tracking. To handle that, the target region is separated to several small blocks, and several groups of samples of the blocks are obtained. We assign the label of different blocks as the way mentioned in Section III-A. Meanwhile, we divide the target candidates in current frame into several blocks as well, and they are used as unlabeled samples of different blocks. Denote $f_H(\mathbf{x}_i)$ and $\{f_B^j(\mathbf{x}_i^j)\}_{j=1}^b$ by the regression values of holistic candidate template $\mathbf{x}_i$ and its corresponding blocks, respectively. Each block classifier f_B^j is trained using the block samples extracted from all the jth blocks of holistic templates, and thus, different block dictionaries will be learned for different classifiers. Finally, the confidence value of a sample $\mathbf{x}_i$ is calculated as

$$f(\mathbf{x}_i) = \nu f_H(\mathbf{x}_i) + (1-\nu)\frac{1}{b}\sum_{j=1}^{b} f_B^j\left(\mathbf{x}_i^j\right) \tag{19}$$

where $\mathbf{x}_i^j$ is the jth block of sample $\mathbf{x}_i$ and ν is the balance weight between holistic candidates and partial candidate templates. Those classifiers are retained every a few frames for computational efficiency. And the sparse codes of samples are obtained by executing (2) using the learned dictionary.

C. Particle Filter Framework

The proposed tracking algorithm is implemented under the particle filter framework. Given the observation $\mathbf{o}_{1:t} = \{\mathbf{o}_i\}_{i=1}^t$ up to time t, the maximum a posterior estimation of object state $\mathbf{s}_t$ can be estimated by

$$\arg\max_{\mathbf{s}_t} p(\mathbf{s}_t \mid \mathbf{o}_{1:t}) \tag{20}$$

which is inferred based on the Bayesian theorem

$$p(\mathbf{s}_t|\mathbf{o}_{1:t}) \propto p(\mathbf{o}_t|\mathbf{s}_t)\int p(\mathbf{s}_t|\mathbf{s}_{t-1})p(\mathbf{s}_{t-1}|\mathbf{o}_{1:t-1})d\mathbf{s}_{t-1} \tag{21}$$

where $p(\mathbf{s}_t|\mathbf{s}_{t-1})$ is the motion model and $p(\mathbf{o}_t|\mathbf{s}_t)$ is the likelihood function. The posterior $p(\mathbf{s}_t|\mathbf{o}_{1:t})$ is approximated by a set of samples $\{\mathbf{s}_t^1, \mathbf{s}_t^2, \ldots, \mathbf{s}_t^N\}$ with their corresponding weights $\{w_t^1, w_t^2, \ldots, w_t^N\}$. The candidates are sampled from a proposal distribution $q(\mathbf{s}_t|\mathbf{s}_{1:t-1}, \mathbf{o}_{1:t}) = p(\mathbf{s}_t|\mathbf{s}_{t-1})$. In our tracking algorithm, the target motion between two consecutive frames is modeled by an affine image warp. And the state $\mathbf{s}_t$ is modeled by $(\xi_x, \xi_y, \theta, s, \eta, \phi)$, where (ξ_x, ξ_y) is the target center coordinate in the image and θ, s, η, and ϕ are the parameters of rotation angle, scale, aspect ratio, and skew, respectively. Without loss of generality, a Gaussian distribution is used to model the motion model with $p(\mathbf{s}_t|\mathbf{s}_{t-1}) = \mathcal{N}(\mathbf{s}_t; \mathbf{s}_{t-1}, \Sigma)$, where Σ is a diagonal covariance matrix.

The likelihood function $p(y_i|\mathbf{s}_i)$ of candidate $\mathbf{x}_i$ is constructed by

$$p(o_i|\mathbf{s}_i) \propto f(\mathbf{x}_i). \tag{22}$$

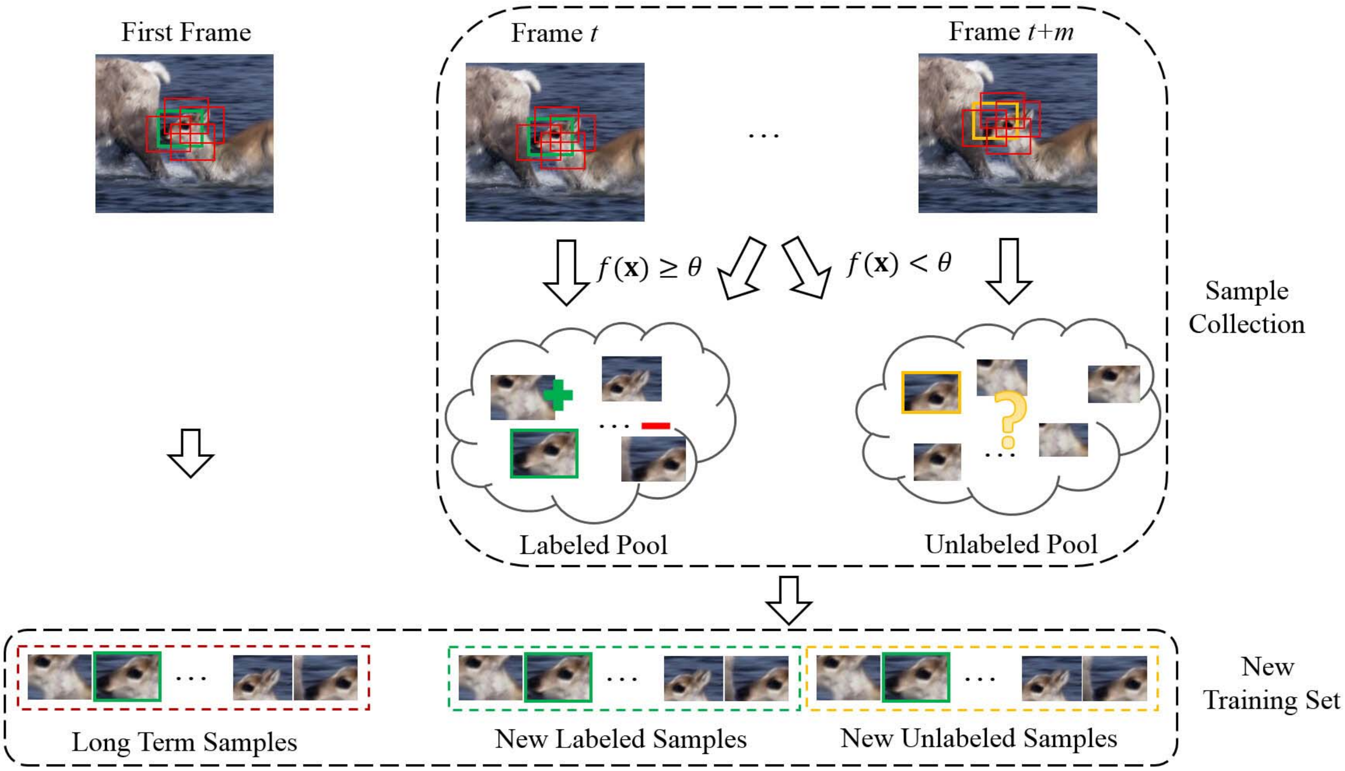

Fig. 3. Updating scheme. The new training sample set is obtained from labeled and unlabeled pools. The samples collected from the first frame are involved in calculation all the time.

The target candidate with highest probability is determined as current estimated target state.

D. Target Redetection

It is common that drifting occurs during long-term tracking and causes tracking failure. Especially, when a target is fully occluded by background, trackers are difficult to locate where a target is, and the estimated targets in these frames are almost random. Therefore, a target redetection algorithm is necessary once the target reappears in new frames. Thus, we introduce the target redetection strategy [27] to handle this problem. Different from [27], we train an support vector machine (SVM) classifier [28] based on the initial target appearance instead of an online random fern classifier [29]. The redetector is activated in case that the maximum response of the target center location is below a predefined threshold τ, which means that tracking fails in the current frame. With this redetection strategy, the performance of our tracker is promoted as we can see in Section IV.

E. Update Strategy

Target appearance changes continuously caused by illumination variations, occlusions, and deformation during tracking. The manifold geometry structure constructed with samples will be different with the changing of appearance. Thus, we should reupdate the dictionary, linear classifiers, and sparse codes to adapt to appearance variation. The target redetector should also be updated.

1) Dictionary Updating: We retain two sample pools, as shown in Fig. 3, during tracking. The labeled samples are stored in the labeled pool, and the unlabeled samples are contained in unlabeled ones. The labeled samples will be cropped based on the current target location and then added into labeled pool when the confidence value of current target is greater than a constant θ. Otherwise, we will consider the candidates in a current frame to be unlabeled samples and place them into unlabeled pool. Then, a certain amount of samples will be selected from these pools randomly every a few frames, and they are regarded as a new training sample set. The discriminative dictionary and classifier will be recalculated by Algorithm 1. To alleviate the pollution of current training set, we remain the samples collected from the first frame in our new training sample set, which is efficient for long-term tracking. The updating scheme is applied on both holistic and block templates.

2) Redetector Updating: In order to get more accurate redetecting results, the redetector should be updated during tracking as well. An online passive-aggressive algorithm [30] is applied to update the SVM redetector using features sampled in the current frame. More details about the online SVM algorithm can be found in [30].

IV. Experiments

The proposed object tracking approach is verified on two challenging tracking benchmarks, including OTB2013 [4] and VOT2015 [31]. We set the number of particles (600) to the same number of these tracking algorithms under framework

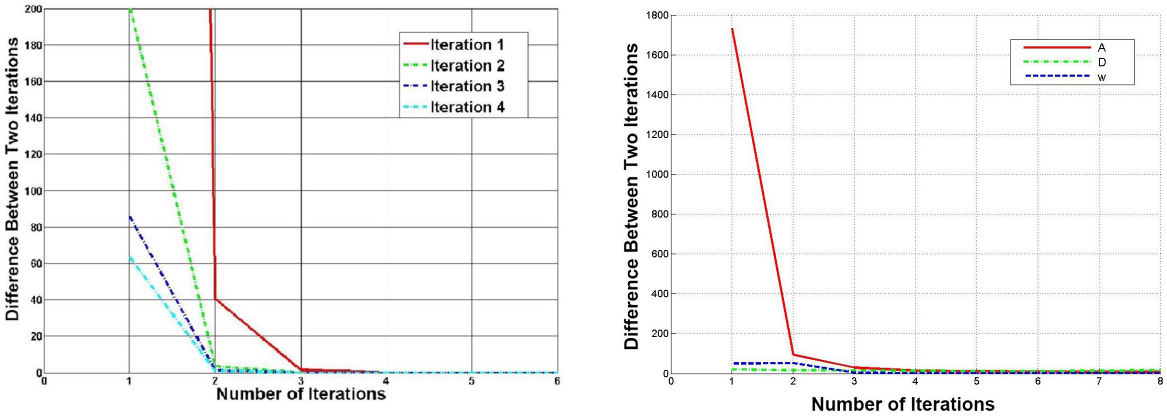

Fig. 4. Left: convergence of our coding algorithm. Right: proposed joint discriminative dictionary, sparse codes, and classifier learning algorithm.

TABLE I
PERFORMANCE SCORES FOR THE POPULAR TRACKERS ON OTB2013

	HDT	DSSM	Struck	FST	CNN-SVM	ODDL	KCF	TGPR	WDL	LNLT	Ours
DP	0.873	0.533	0.654	0.770	0.842	0.561	0.742	0.762	0.689	0.737	0.840
OP	0.594	0.414	0.472	0.547	0.590	0.410	0.516	0.528	0.493	0.508	0.598

of particle filters. The affine parameters of particle filters are set to $[10, 10, 0.04, 0, 0.001, 0]$. The number of positive, negative, and unlabeled samples is set to 20, 200, and 200, respectively, for the proposed learning algorithm. We then intended to separate the holistic template into four parts, which were located in the top-left, top-right, bottom-left, and bottom-right of the template. Thus, the block size was set to half of the template size. We normalize the size of holistic templates to 24×24, and the block size and the step size are set to 12×12 and [12 12], respectively. The number of dictionary items for global templates is 20. The parameters μ, λ_1, and λ_2 in (5) are set to 0.03, 0.09, and 0.1, respectively. The balance factor is set to 0.8 to determine the impact of holistic and block classifiers. We set the threshold $\theta = 0.65$ for pool updating.

A. Implementation Details

We combine the three channels of CIE Lab color features [32] and the histograms of oriented gradients (HOGs) feature [33] of samples as the final template feature vector. The feature in our experiments for each template is a vector combined by the three channels of CIE Lab color features [32] stretched row by row of the target and the HOGs' feature [33] of samples.

The final confidence in (19) of a target candidate is influenced by the weight ν. Thus, some inaccuracy may exist in the center location of the estimated target. To refine the estimated target state, we train a correlation filter [3], [34] using the holistic target template cropped in the initial frame. Different from their methods, the correlation filter is trained using only the target template without any background information in our implementation. Then, once a candidate state is chosen as the state of the current estimated target by (22), we resize the current target as the same size with a target template and calculate a refined center location of confidence response map using the correlation filter learned ahead. The refined center location is determined as the position corresponding to the maximum response in this map. Other parameters, such as rotation angle, scale, aspect ratio, and skew, in the estimated target state are then transferred to the refined target. The correlation filter updating method is the same as [3].

B. Convergence Analysis

To verify the convergence of the proposed globally linear approximation to nonlinear learning algorithm intuitively, the iterations of the proposed algorithm are calculated. To verify the convergence of the coding algorithm with the increase of iteration number, we show the difference between two iterations on the experimental data in Fig. 4 (left). It can be found that the proposed algorithm converges rapidly. In fact, four rounds of iteration are enough for the experiments. Fig. 3 (right) shows the convergence curve of the whole learning algorithm, which is used to calculate the discriminative dictionary, sparse codes, and linear classifier. All of these variables converge rapidly, and eight rounds of iterations are needed at most. The values of these parameters are set to $\mu = 0.03$, $\lambda_1 = 0.09$, and $\lambda_2 = 0.1$ in our experiments.

C. Experimental Results on OTB2013

OTB2013 is a tracking benchmark [4] with 51 videos, where different difficulties encountered in visual tracking are contained. Our tracker is compared with ten popular tracking methods, including Struck [35], KCF [3], FST [38], TGPR [39], two related methods (discriminative sparse similarity map (DSSM) [37] and online discriminative dictionary learning (ODDL) [17]), and two deep learning trackers (convolutional neural network-support vector machine (CNN-SVM) [40], hedged deep tracking (HDT) [42]), and our original version linearization nonlinear learning tracking (LNLT) [23] is

This article has been accepted for inclusion in a future issue of this journal. Content is final as presented, with the exception of pagination.

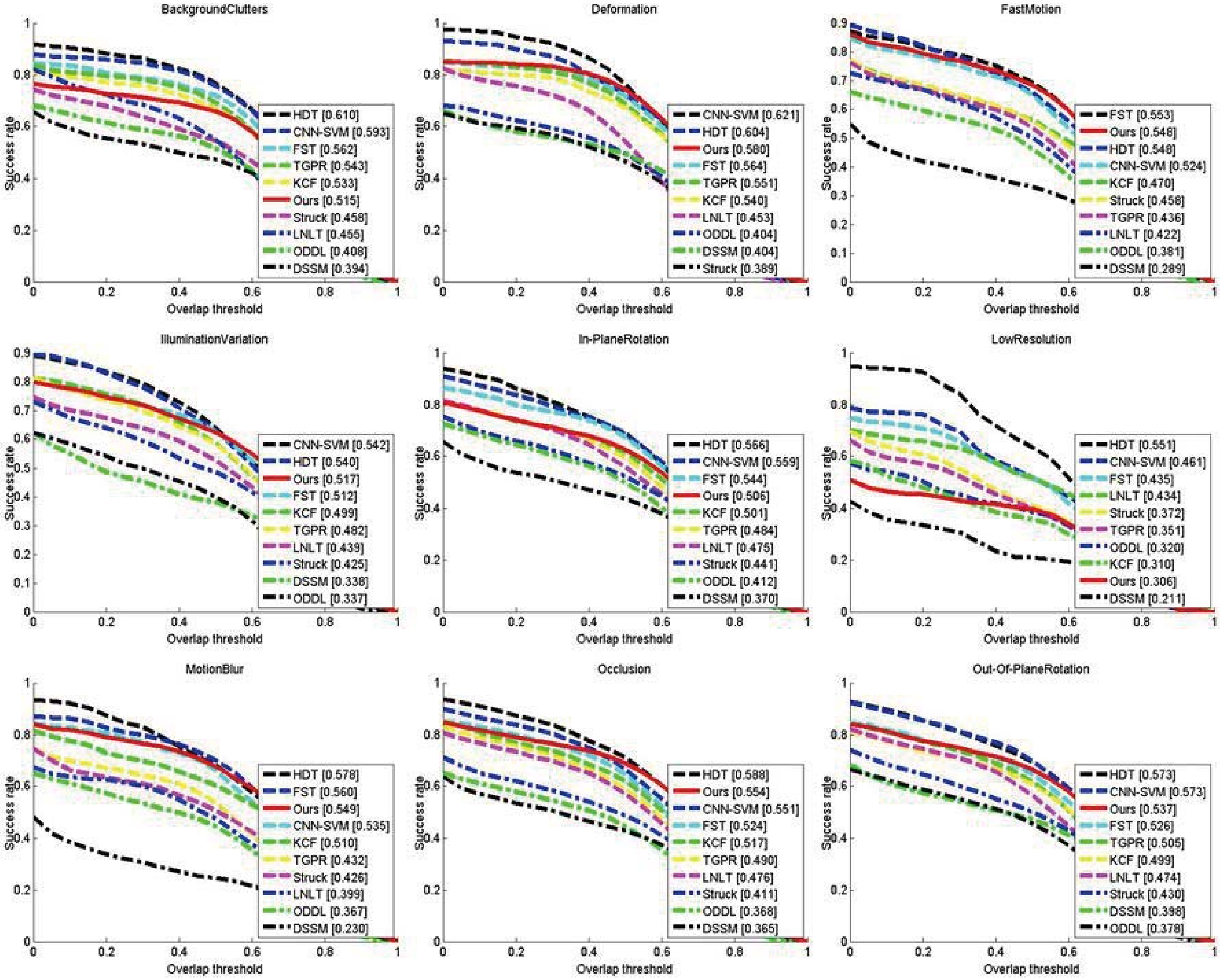

Fig. 5. Attribute-based estimation comparisons of success plots for these trackers.

also included in the comparisons. We apply two measurements, including distance precision (DP) and overlap precision (OP) by one-pass evaluation to evaluate the tracking performance. More details about measurements refer to [4].

1) Overall Estimation: The tracking results of our tracker are compared with those of different popular tracking approaches, and Fig. 1 shows the precision plots and success plots. We collect the center location errors on all sequences of all those tracking methods, and regard the performance scores at 20 pixels as the ranking criterion. The legend of precision plots shows the performance scores. We compute the areas under curves in the success plots as the performance scores of overlap rate. Visual tracking methods based on sparse representation are DSSM and ODDL among these trackers. In precision plots, Struck obtains the best score except for a few other popular tracking methods, which does good work on these image sequences. However, these trackers have no consideration on the embedding manifold spatial structure. Besides, dictionary learning is crucial for tracking methods, and ODDL obtains comparable tracking performance on this benchmark. The proposed tracking approach performs well on the benchmark and even better than the newly proposed works, such as KCF and TGPR. The location error performance score is 0.840, and the overlap performance score is 0.598. In addition, all performance scores of the mentioned trackers are listed in the first two rows of Table I. It verifies the effectiveness of the proposed joint learning algorithm. Those deep learning-based [57] trackers (such as CNN-SVM and HDT) generally learn their classifiers with a large number of training samples from different image data sets. These methods are

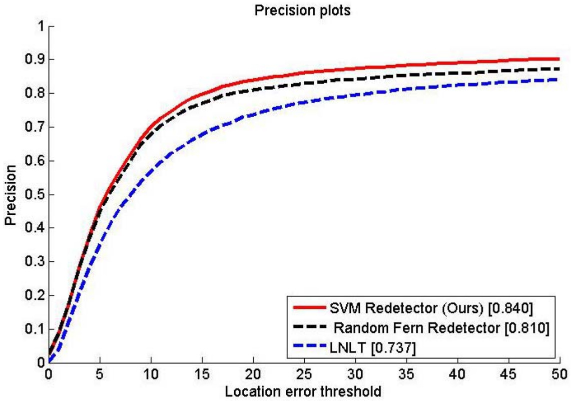

Fig. 6. Comparison results between our tracker using the proposed SVM redetector, our tracker with the random fern redetector [27], and the LNLT tracker [23].

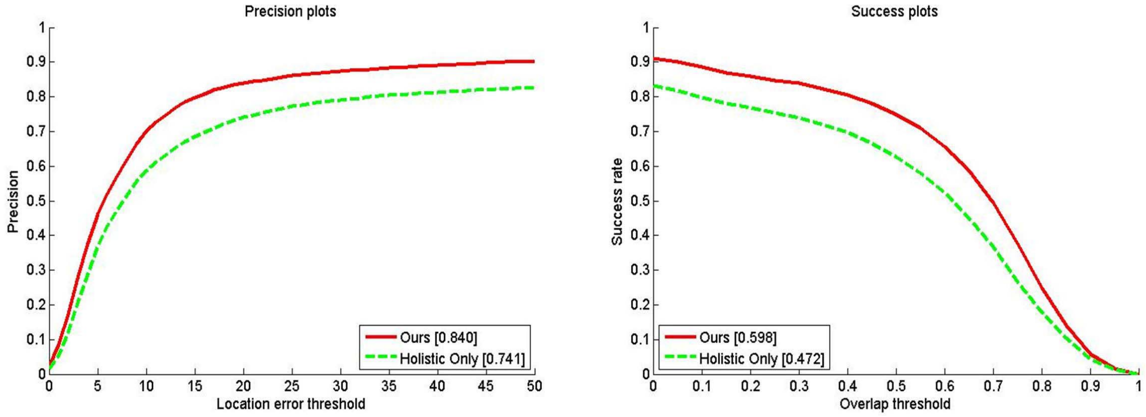

Fig. 7. Experiments comparison between our tracker and the one using holistic template only.

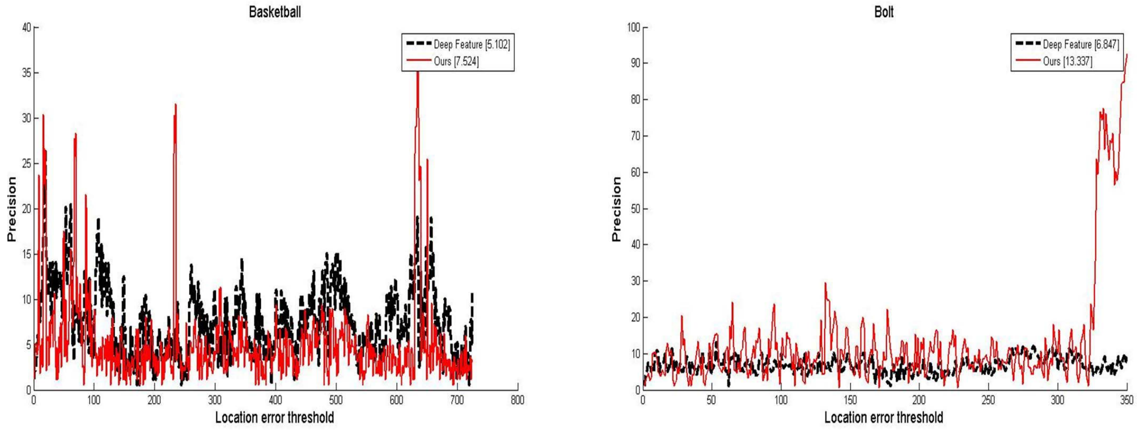

Fig. 8. Experiments with deep features. The average center location errors are shown in the legend.

easy to obtain appearance models with more discriminative power than that in other method, while our method only trains the proposed model with samples from several frames. In spite of this, our tracker still performs comparable results with CNN-SVM and HDT and even better than them according to the overlap evaluation in Fig. 1.

2) *Attributes-Based Estimation:* Different attributes encountered during tracking are annotated for these videos in the benchmark. Eleven attributes, such as background clutters, deformation, fast motion, illumination variation, in-plane rotation, motion blur, occlusion, out-of-plane rotation, low resolution, out-of-view, and scale variation, are designed based on different challenging situations. The performance scores of different tracking methods estimated on this attributes to prove the effectiveness of them. As shown in Fig. 5, the success plots of all tracking algorithms under these challenges are presented in the precision plots. The proposed tracking method performs well on most of these factors.

3) *Analysis of Dictionary Learning:* Our tracker is also compared with ourselves without dictionary learning (WDL) to further prove the validation of discriminative dictionary learning. The parameter setting is consistent with the proposed tracking method. The performance scores of WDL are shown in Table I. The DP and OP of this method are 0.689 and 0.493, respectively, which are inferior to the scores of the proposed tracking approach without target redetection, which are 0.737 and 0.508, respectively. It is observed that the performance of the tracking method with discriminative dictionary learning performs better than the version without discriminative dictionary learning.

4) *Redetector Comparison:* We compare our tracking performances using the introduced redetection method and the random fern redetector used in [27], respectively. As shown in Fig. 6, the DP value of our tracking algorithm on OTB2013 is 84%, which is also better than the one using random fern classifier (81%). Compared with our original tracker (LNLT) [23], the introduced redetection method improves the DP performance about 10%, while the random fern redetector promotes about 8%. Thus, these two redetection methods both improve the final performance.

5) *Effectiveness of Block Classifiers:* We have also tested our tracker with only holistic templates. As shown in Fig. 7, our method with both holistic and block templates achieves a better performance than the one with only holistic target templates. The DP score of our method is higher than that with only holistic templates about 10% and the OP score is higher than that about 12%. Thus, the block classifiers improve the final tracking performance.

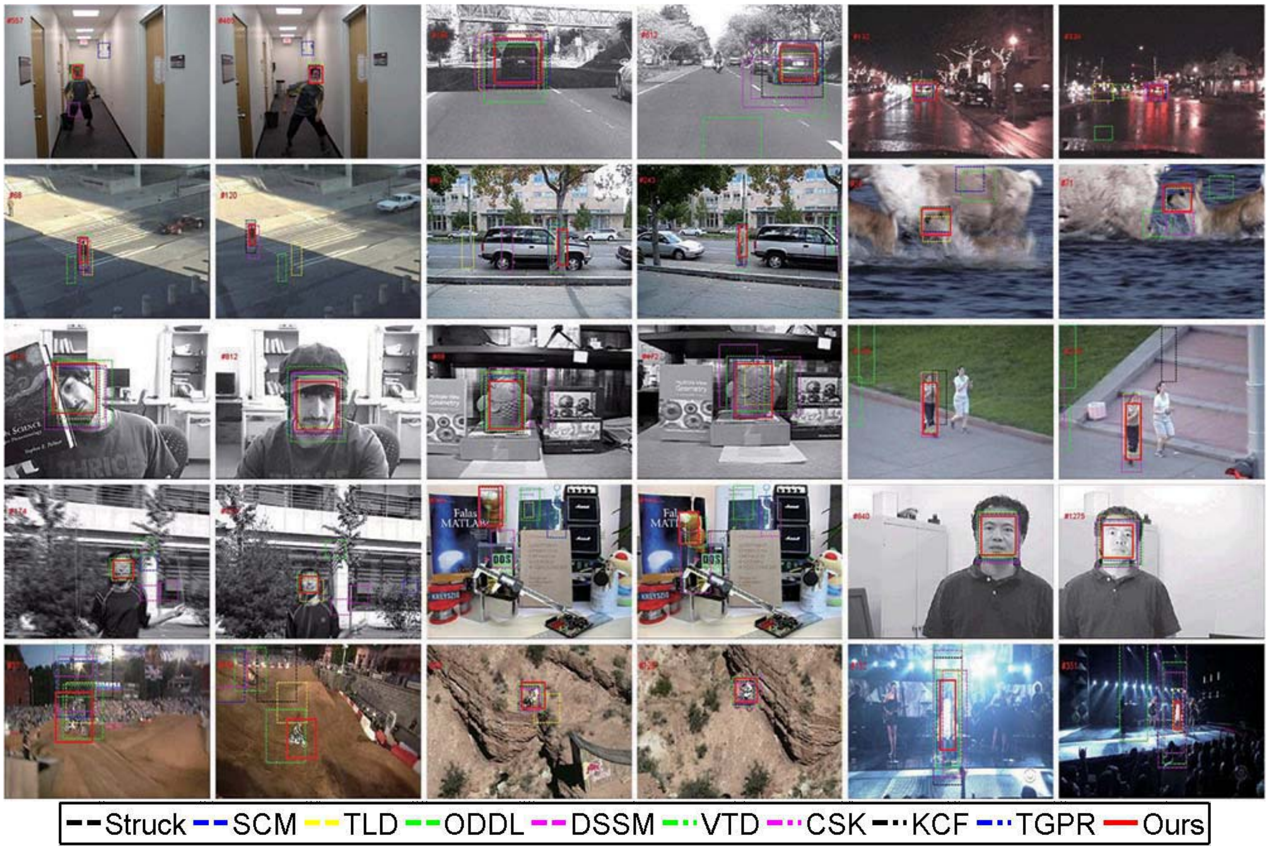

Fig. 9. Visual comparison. These sequences are “Boy,” “Car4,” “CarDark,” “Crossing,” “David3,” “Deer,” “Faceocc2,” “Fish,” “Jogging-1,” “Jumping,” “Lemming,” “Mhyang,” “MotorRolling,” “MountainBike,” and “Singer1” from left to right and top to bottom.

We further test our tracking approach on a more challenging benchmark, the VOT2015 [31]. The performance of our tracker is compared with IVT [44], KCF2 [3], L1APG [13], MDNet [45], MIL [46], MatFlow [48], STC [50], TGPR [39], and Zhang (see [31, A.4]) reported in this benchmark. In these experiments, each tracker is initialized with the ground truth bounding box, and it is also initialized by a perturbed bounding box centered around the ground truth bounding box randomly. The estimation toolkit[2] reports the final tracking results, including accuracy and robustness. The accuracy measures the bounding box overlap ratio with ground truth, and the robustness assesses the number of failures that indicate when the overlap measure equals zero. As shown in Fig. 2, we compare our tracking method with 16 popular tracking approaches in VOT2015 by the expected overlap curves, scores, and AR plots of all these trackers. Our method performs better than these popular trackers on this more challenging data set.

D. More Experiments and Visual Comparisons

1) Experiments With Deep Features: We have also applied the deep feature to our method. We extract convolutional feature from ResNet [57] for each particle, including holistic and block templates. The pertained ResNet model “imagenet-resnet-50-dag” is used as deep features. Under the particle filter tracking framework, the computational complexity is related to the particle numbers. Two video clips, including “Basketball” and “Bolt,” are randomly tested to verify the effectiveness of deep feature. As shown in Fig. 8, deep feature improves the tracking performance. However, the average tracking speed of the deep feature version is 1200 s/frame, while our original tracking speed is about 3 s/frame. Our method is much faster than the one with deep feature.

We further show a part of the tracking results obtained by the proposed tracking approach and other trackers in Fig. 9. In the “Car4,” “CarDark,” and “Singer1” sequences from OTB2013, the illumination of these targets changes drastically. Benefiting from the discriminative appearance model, the proposed tracker is robust to illumination changes and can track these targets all the time. In “David3” and “Faceocc2,” we show the tracking results on the videos where targets are confronted with heavy global and partial occlusions. For example, in “David3,” the pedestrian suffers from global occlusion when he walks behind a tree (#83). TLD and CXT fail to track the target even when he is occluded by a lamp pole (#24). Struck and SCM also fail after the pedestrian walks away from the tree (#141). Only our tracker and TGPR could track the pedestrian in the whole sequence successfully. The appearances of some targets change caused by scale variation, such as “Singer1.”

[2] http://www.votchallenge.net/vot2015/

V. Conclusion

Based on the theory of globally linear approximations to nonlinear learning, a principled method has been presented to learn sparse codes, discriminative dictionary, and nonlinear classifier jointly for visual tracking. We then introduce an optimization algorithm to calculate the discriminative dictionary, sparse codes, and classifier iteratively. We develop a visual tracking method under the particle filter framework and adopt an online updating scheme to adapt to target appearance changes. To further improve the tracking performance, the target redetection strategy is introduced. Experiments on challenging video clips demonstrate the superior performance of the proposed method in comparison with popular trackers. In the future, we will attempt to extend our method to multiple target tracking with multitask spare learning [56].

Appendix A
Derivations of Subproblem B

The approximated objective function can be written as

$$\begin{aligned}\min_{\mathbf{A}}\ & \sum_{i=1}^{u+n}\left(\|\mathbf{x}_i-\mathbf{D}\boldsymbol{\alpha}_i\|^2+\mu\|\mathbf{c}_i\odot\boldsymbol{\alpha}_i\|^2\right)\\ & +\lambda_1\left\|\mathbf{A}_l^T\mathbf{w}-\mathbf{y}\right\|^2+\lambda_3\sum_{i=1}^{n+u}\sum_{j=1}^{n+u}\|\boldsymbol{\alpha}_i-\boldsymbol{\alpha}_j\|^2B_{ij}\\ \text{s.t.}\ & \sum_{j=1}^{m}\boldsymbol{\alpha}_i^j=1,\quad i=1,\ldots,n,n+1,\ldots,n+u\end{aligned}$$

where $\mathbf{c_i}$ represents the distance vector composed by the ith sample and all the dictionary items with its jth elements $\mathbf{c}_i^j=\|\mathbf{x}_i-\mathbf{d}_j\|$.

Let

$$\begin{aligned}f=&\sum_{i=1}^{u+n}\left(\|\mathbf{x}_i-\mathbf{D}\boldsymbol{\alpha}_i\|^2+\mu\|\operatorname{diag}(\mathbf{c}_i)\boldsymbol{\alpha}_i\|^2\right)\\ &+\lambda_1\sum_{i}^{n}\left\|\boldsymbol{\alpha}_i^T\mathbf{w}-y_i\right\|^2+\nu\left(\sum_{i=1}^{n+u}\left(\boldsymbol{\alpha}_i^T\mathbf{1}-1\right)\right)\\ &+\lambda_3\sum_{i=1}^{n+u}\sum_{j=1}^{n+u}\|\boldsymbol{\alpha}_i-\boldsymbol{\alpha}_j\|^2B_{ij}.\end{aligned}$$

When $i\le n$, we take the derivative of f with respect to $\boldsymbol{\alpha}_i$. Namely,

$$\begin{aligned}\frac{\partial f}{\partial\boldsymbol{\alpha}_i}=&\ 2\mathbf{D}^T(\mathbf{D}\boldsymbol{\alpha}_i-\mathbf{x}_i)+2\mu\operatorname{diag}(\mathbf{c}_i^2)\boldsymbol{\alpha}_i+2\lambda_1\mathbf{w}(\mathbf{w}^T\boldsymbol{\alpha}_i-y_i)\\ &+4\lambda_3\sum_{j=1}^{n+u}(\boldsymbol{\alpha}_i-\boldsymbol{\alpha}_j)B_{ij}+\nu\mathbf{1}.\end{aligned}$$

Let the derivation be zero, and we denote

$$\mathbf{P}=\mathbf{D}^T\mathbf{D}+\mu\operatorname{diag}(\mathbf{c}_i^2)+\lambda_1\mathbf{w}\mathbf{w}^T+2\lambda_3\sum_{j=1}^{n+u}B_{ij}$$

$$\mathbf{Q}=\mathbf{D}^T\mathbf{x}_i+\lambda_1\mathbf{w}y_i+2\lambda_3\sum_{j=1}^{n+u}\boldsymbol{\alpha}_jB_{ij}.$$

We can get the result of $\boldsymbol{\alpha}_i$ as

$$\boldsymbol{\alpha}_i=\mathbf{P}^{-1}\left(\mathbf{Q}-\frac{\mathbf{1}^T\mathbf{P}^{-1}\mathbf{Q}\mathbf{1}-1}{\mathbf{1}^T\mathbf{P}^{-1}\mathbf{1}}\mathbf{1}\right).$$

When $i>n$,

$$\mathbf{P}=\mathbf{D}^T\mathbf{D}+\mu\operatorname{diag}(\mathbf{c}_i^2)+2\lambda_3\sum_{j=1}^{n+u}B_{ij}$$

$$\mathbf{Q}=\mathbf{D}^T\mathbf{x}_i+2\lambda_3\sum_{j=1}^{n+u}\boldsymbol{\alpha}_jB_{ij}.$$

Appendix B
Derivations of Subproblem C

The original problem is equivalent to

$$\begin{aligned}&\min_{\mathbf{D}}\sum_{i=1}^{n+u}\left(\|\mathbf{x}_i-\mathbf{D}\boldsymbol{\alpha}_i\|^2+\mu\sum_{j=1}^{m}|\alpha_i^j|\|\mathbf{d}_j-\mathbf{x}_i\|^2\right)\\ &\Rightarrow\min_{\mathbf{D}}\sum_{i=1}^{n+u}\left(\boldsymbol{\alpha}_i^T\mathbf{D}^T\mathbf{D}\boldsymbol{\alpha}_i-2\mathbf{x}_i^T\mathbf{D}\boldsymbol{\alpha}_i+\mu\sum_{j=1}^{m}|\alpha_i^j|\right.\\ &\qquad\qquad\left.(\mathbf{d}_j^T\mathbf{d}_j-2\mathbf{x}_i^T\mathbf{d}_j)\right)\\ &\Rightarrow\min_{\mathbf{D}}\sum_{i=1}^{n+u}\left(\operatorname{tr}(\mathbf{D}^T\mathbf{D}\boldsymbol{\alpha}_i\boldsymbol{\alpha}_i^T)-2\operatorname{tr}(\mathbf{D}^T\mathbf{x}_i\boldsymbol{\alpha}_i^T).\right.\\ &\qquad\left.+\mu\operatorname{tr}(\mathbf{D}^T\mathbf{D}\operatorname{diag}(|\boldsymbol{\alpha}_i|))-2\mu\operatorname{tr}(\mathbf{D}^T\mathbf{x}_i|\boldsymbol{\alpha}_i|^T)\right)\\ &\Rightarrow\min_{\mathbf{D}}\operatorname{tr}\left(\mathbf{D}^T\mathbf{D}\sum_{i=1}^{n+u}\left(\boldsymbol{\alpha}_i\boldsymbol{\alpha}_i^T+\mu\operatorname{diag}(|\boldsymbol{\alpha}_i|)\right)\right)\\ &\qquad-2\operatorname{tr}\left(\mathbf{D}^T\sum_{i=1}^{n+u}\left(\mathbf{x}_i\boldsymbol{\alpha}_i^T+\mu\mathbf{x}_i|\boldsymbol{\alpha}_i|^T\right)\right).\end{aligned}$$

Let us denote

$$\mathbf{G}=\sum_{i=1}^{n+u}\left(\boldsymbol{\alpha}_i\boldsymbol{\alpha}_i^T+\mu\operatorname{diag}(|\boldsymbol{\alpha}_i|)\right)$$

$$\mathbf{S}=\sum_{i=1}^{n+u}\left(\mathbf{x}_i\boldsymbol{\alpha}_i^T+\mu\mathbf{x}_i|\boldsymbol{\alpha}_i|^T\right).$$

By substituting $\mathbf{G}$ and $\mathbf{S}$ in the above equation, the original objective is equivalent to minimizing

$$\min_{\mathbf{D}}\operatorname{tr}(\mathbf{D}^T\mathbf{D}\mathbf{G})-2\operatorname{tr}(\mathbf{D}^T\mathbf{S}).$$

The minimization problem has a closed-form solution by setting the derivative of the above equation to zero. Finally, we get the final solution

$$\mathbf{D}=\mathbf{S}\mathbf{G}^{-1}.$$

References

[1] H. Yang, L. Shao, F. Zheng, L. Wang, and Z. Song, "Recent advances and trends in visual tracking: A review," *Neurocomputing*, vol. 74, no. 18, pp. 3823–3831, Nov. 2011.

[2] A. W. M. Smeulders, D. M. Chu, R. Cucchiara, S. Calderara, A. Dehghan, and M. Shah, "Visual tracking: An experimental survey," *IEEE Trans. Pattern Anal. Mach. Intell.*, vol. 36, no. 7, pp. 1442–1468, Jul. 2014.

[3] J. F. Henriques, R. Caseiro, P. Martins, and J. Batista, "High-speed tracking with kernelized correlation filters," *IEEE Trans. Pattern Anal. Mach. Intell.*, vol. 37, no. 3, pp. 583–596, Mar. 2015.

[4] Y. Wu, J. Lim, and M.-H. Yang, "Online object tracking: A benchmark," in *Proc. IEEE Conf. Comput. Vis. Pattern Recognit.*, Jun. 2013, pp. 2411–2418.

[5] M. Kristan *et al.*, "The visual object tracking vot2014 challenge results," in *Proc. Eur. Conf. Comput. Vis. Workshops*, 2014, pp. 191–217.

[6] Z. Jiang, Z. Lin, and L. S. Davis, "Learning a discriminative dictionary for sparse coding via label consistent K-SVD," in *Proc. IEEE Conf. Comput. Vis. Pattern Recognit.*, Jun. 2011, pp. 1697–1704.

[7] S. Zhang, H. Yao, X. Sun, and X. Lu, "Sparse coding based visual tracking: Review and experimental comparison," *Pattern Recognit.*, vol. 46, no. 7, pp. 1772–1788, Jul. 2013.

[8] M. Yang, L. Zhang, X. Feng, and D. Zhang, "Fisher discrimination dictionary learning for sparse representation," in *Proc. IEEE Int. Conf. Comput. Vis.*, Nov. 2011, pp. 543–550.

[9] L. Shao, L. Liu, and X. Li, "Feature learning for image classification via multiobjective genetic programming," *IEEE Trans. Neural Netw. Learn. Syst.*, vol. 25, no. 7, pp. 1359–1371, Jul. 2014.

[10] L. Liu and L. Shao, "Sequential compact code learning for unsupervised image hashing," *IEEE Trans. Neural Netw. Learn. Syst.*, vol. 27, no. 12, pp. 2526–2536, Dec. 2016.

[11] X. Mei and H. Ling, "Robust visual tracking using ℓ_1 minimization," in *Proc. IEEE Int. Conf. Comput. Vis.*, Dec. 2009, pp. 1436–1443.

[12] J. Shen, X. Yang, Y. Jia, and X. Li, "Intrinsic images using optimization," in *Proc. IEEE Conf. Comput. Vis. Pattern Recognit.*, Jun. 2011, pp. 3481–3487.

[13] C. Bao, Y. Wu, H. Ling, and H. Ji, "Real time robust ℓ_1 tracker using accelerated proximal gradient approach," in *Proc. IEEE Conf. Comput. Vis. Pattern Recognit.*, Jun. 2012, pp. 1830–1837.

[14] W. Zhong, H. Lu, and M.-H. Yang, "Robust object tracking via sparsity-based collaborative model," in *Proc. IEEE Conf. Comput. Vis. Pattern Recognit.*, Jun. 2012, pp. 1838–1845.

[15] X. Lu, Y. Yuan, and P. Yan, "Robust visual tracking with discriminative sparse learning," *Pattern Recognit.*, vol. 46, no. 7, pp. 1762–1771, Jul. 2013.

[16] J. Shen, X. Yang, X. Li, and Y. Jia, "Intrinsic image decomposition using optimization and user scribbles," *IEEE Trans. Cybern.*, vol. 43, no. 2, pp. 425–436, Apr. 2013.

[17] F. Yang, Z. Jiang, and L. S. Davis, "Online discriminative dictionary learning for visual tracking," in *Proc. IEEE Winter Conf. Appl. Comput. Vis.*, Mar. 2014, pp. 854–861.

[18] K. Yu, T. Zhang, and Y. Gong, "Nonlinear learning using local coordinate coding," in *Proc. Adv. Neural Inf. Process. Syst.*, 2009, pp. 2223–2231.

[19] K. Yu and T. Zhang, "Improved local coordinate coding using local tangents," in *Proc. Int. Conf. Mach. Learn.*, 2010, pp. 1215–1222.

[20] J. Wang, J. Yang, K. Yu, F. Lv, T. Huang, and Y. Gong, "Locality-constrained linear coding for image classification," in *Proc. IEEE Conf. Comput. Vis. Pattern Recognit.*, Jun. 2010, pp. 3360–3367.

[21] Y. Lin *et al.*, "Large-scale image classification: Fast feature extraction and svm training," in *Proc. IEEE Conf. Comput. Vis. Pattern Recognit.*, Jun. 2011, pp. 1689–1696.

[22] B. Xie, M. Song, and D. Tao, "Large-scale dictionary learning for local coordinate coding," in *Proc. Brit. Mach. Vis. Conf.*, 2010, pp. 1–9.

[23] B. Ma, H. Hu, J. Shen, Y. Zhang, and F. Porikli, "Linearization to nonlinear learning for visual tracking," in *Proc. IEEE Int. Conf. Comput. Vis.*, Dec. 2015, pp. 4400–4407.

[24] W. Wang, J. Shen, X. Li, and F. Porikli, "Robust video object cosegmentation," *IEEE Trans. Image Process.*, vol. 24, no. 10, pp. 3137–3148, Oct. 2015.

[25] M. Belkin, P. Niyogi, and V. Sindhwani, "Manifold regularization: A geometric framework for learning from labeled and unlabeled examples," *J. Mach. Learn. Res.*, vol. 7, pp. 2399–3434, Nov. 2006.

[26] X. Dong, J. Shen, D. Yu, W. Wang, J. Liu, and H. Huang, "Occlusion-aware real-time object tracking," *IEEE Trans. Multimedia*, vol. 19, no. 4, pp. 763–771, Apr. 2017.

[27] C. Ma, X. Yang, C. Zhang, and M.-H. Yang, "Long-term correlation tracking," in *Proc. IEEE Conf. Comput. Vis. Pattern Recognit.*, Jun. 2015, pp. 5388–5396.

[28] J. A. K. Suykens and J. Vandewalle, "Least squares support vector machine classifiers," *Neural Process. Lett.*, vol. 9, no. 3, pp. 293–300, Jun. 1999.

[29] Z. Kalal, K. Mikolajczyk, and J. Matas, "Tracking-learning-detection," *IEEE Trans. Pattern Anal. Mach. Intell.*, vol. 34, no. 7, pp. 1409–1422, Jul. 2012.

[30] K. Crammer, O. Dekel, J. Keshet, S. Shalev-Shwartz, and Y. Singer, "Online passive-aggressive algorithms," *J. Mach. Learn. Res.*, vol. 7, pp. 551–585, Dec. 2006.

[31] M. Kristan *et al.*, "The visual object tracking VOT2015 challenge results," in *Proc. IEEE Int. Conf. Comput. Vis. Workshop (ICCVW)*, Dec. 2015, pp. 564–586.

[32] M. D. Fairchild, *Color Appearance Models*. Hoboken, NJ, USA: Wiley, 2013.

[33] P. F. Felzenszwalb, R. B. Girshick, D. McAllester, and D. Ramanan, "Object detection with discriminatively trained part-based models," *IEEE Trans. Pattern Anal. Mach. Intell.*, vol. 32, no. 9, pp. 1627–1645, Sep. 2010.

[34] J. F. Henriques, R. Caseiro, P. Martins, and J. Batista, "Exploiting the circulant structure of tracking-by-detection with kernels," in *Proc. Eur. Conf. Comput. Vis.*, 2012, pp. 702–715.

[35] S. Hare, A. Saffari, and P. H. Torr, "Struck: Structured output tracking with kernels," in *Proc. IEEE Int. Conf. Comput. Vis.*, Dec. 2011, pp. 263–270.

[36] J. Shen, Y. Du, W. Wang, and X. Li, "Lazy random walks for superpixel segmentation," *IEEE Trans. Image Process.*, vol. 23, no. 4, pp. 1451–1462, Apr. 2014.

[37] B. Zhuang, H. Lu, Z. Xiao, and D. Wang, "Visual tracking via discriminative sparse similarity map," *IEEE Trans. Image Process.*, vol. 23, no. 4, pp. 1872–1881, Apr. 2014.

[38] S. Zhang, S. Zhao, Y. Sui, and L. Zhang, "Single object tracking with fuzzy least squares support vector machine," *IEEE Trans. Image Process.*, vol. 24, no. 12, pp. 5723–5738, Dec. 2015.

[39] J. Gao, H. Ling, W. Hu, and J. Xing, "Transfer learning based visual tracking with Gaussian processes regression," in *Proc. Eur. Conf. Comput. Vis.*, 2014, pp. 188–203.

[40] S. Hong, T. You, S. Kwak, and B. Han, "Online tracking by learning discriminative saliency map with convolutional neural network," in *Proc. Int. Conf. Mach. Learn.*, 2015, pp. 597–606.

[41] W. Wang, J. Shen, and F. Porikli, "Saliency-aware geodesic video object segmentation," in *Proc. IEEE Conf. Comput. Vis. Pattern Recognit.*, Jun. 2015, pp. 3395–3402.

[42] Y. Qi, S. Zhang, L. Qin, H. Yao, Q. Huang, J. Lim, and M.-H. Yang, "Hedged deep tracking," in *Proc. IEEE Conf. Comput. Vis. Pattern Recognit.*, Jun. 2016, pp. 4303–4311.

[43] B. Ma, L. Huang, J. Shen, L. Shao, M.-H. Yang, and F. Porikli, "Visual tracking under motion blur," *IEEE Trans. Image Process.*, vol. 25, no. 12, pp. 5867–5876, Dec. 2016.

[44] D. A. Ross, J. Lim, R.-S. Lin, and M.-H. Yang, "Incremental learning for robust visual tracking," *Int. J. Comput. Vis.*, vol. 77, nos. 1–3, pp. 125–141, 2008.

[45] H. Nam and B. Han, "Learning multi-domain convolutional neural networks for visual tracking," in *Proc. IEEE Conf. Comput. Vis. Pattern Recognit.*, Jun. 2016, pp. 4293–4302.

[46] B. Babenko, M.-H. Yang, and S. Belongie, "Robust object tracking with online multiple instance learning," *IEEE Trans. Pattern Anal. Mach. Intell.*, vol. 33, no. 8, pp. 1619–1632, Aug. 2011.

[47] B. Ma, H. Hu, J. Shen, Y. Liu, and L. Shao, "Generalized pooling for robust object tracking," *IEEE Trans. Image Process.*, vol. 25, no. 9, pp. 4199–4208, Sep. 2016.

[48] M. E. Maresca and A. Petrosino, "Matrioska: A multi-level approach to fast tracking by learning," in *Proc. Int. Conf. Image Anal. Process.*, 2013, pp. 419–428.

[49] B. Ma, L. Huang, J. Shen, and L. Shao, "Discriminative tracking using tensor pooling," *IEEE Trans. Cybern.*, vol. 46, no. 11, pp. 2411–2422, Nov. 2016.

[50] K. Zhang, L. Zhang, Q. Liu, D. Zhang, and M.-H. Yang, "Fast visual tracking via dense spatio-temporal context learning," in *Proc. Eur. Conf. Comput. Vis.*, 2014, pp. 127–141.

[51] S. I. Yu, Y. Yang, and A. Hauptmann, "Harry potter's marauder's map: Localizing and tracking multiple persons-of-interest by nonnegative discretization," *IEEE Comput. Vis. Pattern Recognit.*, Jun. 2013, pp. 3714–3720.

[52] B. Ma, J. Shen, Y. Liu, H. Hu, L. Shao, and X. Li, "Visual tracking using strong classifier and structural local sparse descriptors," *IEEE Trans. Multimedia*, vol. 17, no. 10, pp. 1818–1828, Oct. 2015.

[53] Y. Yang, F. Nie, D. Xu, J. Luo, Y. Zhuang, and Y. Pan, "A multimedia retrieval framework based on semi-supervised ranking and relevance feedback," *IEEE Trans. Pattern Anal. Mach. Intell.*, vol. 34, no. 4, pp. 723–742, Apr. 2012.

[54] J. Shen, D. Yu, L. Deng, and X. Dong, "Fast online tracking with detection refinement," *IEEE Trans. Intell. Transp. Syst.*, to be published, doi: 10.1109/TITS.2017.2750082.

[55] L. Huang, B. Ma, J. Shen, L. Shao, and F. Porikli, "Visual tracking by sampling in part space," *IEEE Trans. Image Process.*, vol. 26, no. 12, pp. 5800–5810, Dec. 2017.

[56] Y. Yang, Z. Ma, A. G. Hauptmann, and N. Sebe, "Feature selection for multimedia analysis by sharing information among multiple tasks," *IEEE Trans. Multimedia*, vol. 15, no. 3, pp. 661–669, Apr. 2013.

[57] K. He, X. Zhang, S. Ren, and J. Sun, "Deep residual learning for image recognition," in *Proc. IEEE Comput. Vis. Pattern Recognit.*, Jun. 2015, pp. 770–778.

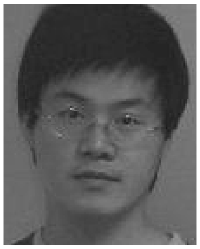

Bo Ma received the Ph.D. degree in computer science from the Harbin Institute of Technology, Harbin, China, in 2003.

In 2006, he joined the Department of Computer Science, Beijing Institute of Technology, Beijing, China, where he is currently an Associate Professor. He has published about 40 journal and conference papers, such as the IEEE Transactions on Image Processing and the IEEE International Conference on Computer Vision. His current research interests include statistical pattern recognition and computer vision.

Hongwei Hu is currently pursuing the Ph.D. degree with the School of Computer Science, Beijing Institute of Technology, Beijing, China.

His current research interests include visual object tracking algorithms.

Jianbing Shen (M'11–SM'12) is currently a Professor with the School of Computer Science, Beijing Institute of Technology, Beijing, China. He has published about 70 journal and conference papers, such as the IEEE Transactions on Pattern Analysis and Machine Intelligence, the IEEE Transactions on Image Processing, the IEEE Conference on Computer Vision and Pattern Recognition, and the IEEE International Conference on Computer Vision. His current research interests include computer vision and machine learning.

Mr. Shen serves as an Associate Editor for *Neurocomputing* journal.

Yuping Zhang is currently pursuing the Ph.D. degree with the School of Computer Science, Beijing Institute of Technology, Beijing, China.

His current research interests include efficient visual object tracking in videos.

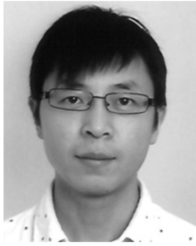

Ling Shao (M'09–SM'10) is currently the Chief Scientist of JD Artificial Intelligence Research, Beijing, China, and is also a Professor with the School of Computing Sciences, University of East Anglia, Norwich, UK. His current research interests include computer vision, image processing, pattern recognition, and machine learning.

Dr. Shao is a fellow of the IET. He is an Associate Editor of the IEEE Transactions on Image Processing and the IEEE Transactions on Neural Networks and Learning Systems.

Fatih Porikli (F'13) is currently a Professor with the Research School of Engineering, Australian National University, Canberra, ACT, Australia. He has contributed broadly to object and motion tracking, and video analytics.

Prof. Porikli was a recipient of the R&D 100 Scientist of the Year Award in 2006. He has received four best paper awards at premier IEEE conferences, including the Best Paper Runner-Up at the IEEE Conference on Computer Vision and Pattern Recognition. He serves as the Associate Editor for five premier journals, including the *IEEE Signal Processing Magazine* and the IEEE Transactions on Multimedia.